

Regularization dependence of $S = 0$ and $S = -1$ meson-baryon system in the chiral unitary model

S.I.Nam,^{1,2,*} H.-Ch.Kim,^{2,†} T.Hyodo,^{1,‡} D.Jido,^{3,§} and A.Hosaka^{1,¶}

¹*Research Center for Nuclear Physics (RCNP), Ibaraki, Osaka 567-0047, Japan*

²*Department of Physics, Pusan National University, Busan 609-735, Korea*

³*ECT*, Villa Tambosi, Strada delle Tabarelle 286, I-38050 Villazzano (Trento), Italy*

(Dated: December 3, 2021)

Abstract

We investigate the dependence of s-wave meson-baryon scattering amplitudes on different regularizations within the framework of the chiral unitary model. We employ two different regularization schemes, *i.e.* dimensional and form-factor regularizations to tame the divergences in the model. We also study the analytic structures of T -matrices, using those regularization schemes. We find that while the form-factor regularization produces almost the same results as the dimensional regularization did, the on-shell approximation is to some extent limited in the case of the form-factor regularization. Having chosen parameters properly, we show that the regularization dependences can be minimized.

PACS numbers: 13.75.Gx, 13.75.Jz, 13.85.Fb, 14.20.Gk

Keywords: Meson-baryon scattering, the chiral unitary model, regularization

*Electronic address: sinam@rcnp.osaka-u.ac.jp

†Electronic address: hchkim@pusan.ac.kr

‡Electronic address: hyodo@rcnp.osaka-u.ac.jp

§Electronic address: jido@ect.it

¶Electronic address: hosaka@rcnp.osaka-u.ac.jp

I. INTRODUCTION

Understanding meson-baryon scattering has been a very important issue for several decades, since it gives information not only on the strong interaction between hadrons but also on the origin of baryonic resonances. Recently, chiral perturbation theory has been of great success in explaining low-energy meson-baryon scattering, in particular, strangeness $S = 0, -1$ channels. While S -wave πN and $K^+ N$ scattering can be well described by the Lagrangian of leading order in the chiral expansion, the $\bar{K} N$ system requires multi-coupled channels in order to generate resonances such as $\Lambda(1405)$ [1, 2]. Though chiral perturbation theory (ChPT) provides us with a theoretical and systematic framework to study meson-baryon systems, it is restricted to lower energy regimes. In order to explain the $\bar{K} N$ system quantitatively, one has to go beyond ChPT.

Recently, there have been noticeable works on the $\bar{K} N$ systems, based on the effective chiral Lagrangian: Kaiser *et al.* [3] examined the S -wave $\bar{K} N$ system. They utilized three different types of the pseudo-potentials, keeping the low energy constants from the effective chiral Lagrangian and solved the Lippmann-Schwinger (LS) equation in the coupled-channel formalism. Krippa and Londergen [4] investigated also $\bar{K} N$ scattering, using the on-shell approximation. Though Ref. [4] seems to describe the experimental data [5, 6] well, threshold behavior can not be reproduced well in the $\Sigma^- \pi^+$, $\Sigma^+ \pi^-$, and $\Lambda \pi^0$ channels due to the openings of new channels. The Valencia group also studied extensively the s -wave $\bar{K} N$ system [7]. Ref. [7] started from the effective chiral Lagrangian to construct the pseudo-potentials and used the on-shell factorization to solve the coupled-channel LS equation, employing a regularization with the three-dimensional cut-off. Later, [8] introduced the dimensional regularization instead of the three dimensional cut-off. They also made use of the N/D method to solve the scattering equation. Lutz and Kolomeitsev [9] investigated meson-baryon scattering in the context of the effective chiral Lagrangian with the large N_c counting. They introduced a minimal chiral subtraction scheme within the dimensional regularization in order to keep the covariant chiral counting rules. Though there exist technical differences between these works, almost all these works showed a remarkable agreement with experimental data. Thus, it is of great significance to understand some essence, if any, in dynamics of different technical methods, in particular, different regularization schemes and the role of corresponding parameters.

In the present work, we turn our attention to the dependence of the s -wave $\bar{K}N$ and πN systems on different regularization schemes. While the dimensional regularization is preferably selected in ChPT, the conventional meson-exchange model [10, 11] gets used to introduce form factors, which describe the extended hadron structure, as a regularization. Though the dimensional regularization gains an advantage over the form factors in many aspects, in particular, in the context of renormalization and gauge invariance, it is less convenient to associate with a LS-type scattering equation. Hence, in this work, we will show that the use of form factors presents almost the same results as that of the dimensional regularization. The present investigation will shed light on the meaning of the parameters involved in the regularization and will pave the way for solving the LS scattering equation without on-shell approximation in the future work by employing the form factors in place of the dimensional regularization.

The paper is organized as follows: In section II, we shall explain the formalism of the chiral unitary model to investigate the meson-baryon systems. The analytic structure of the scattering amplitudes will be presented. In section III, we shall give the numerical results in the $S = 0$ channel with two different regularizations used. In section IV, we shall present those in the $S = -1$ channel. In section V, we shall summarize the present work and draw conclusion with outlook.

II. FORMALISM

We start with the effective chiral Lagrangian to the lowest order \mathcal{L}_{MB}^1 [12]:

$$\begin{aligned}\mathcal{L}_{MB}^1 = & \langle \bar{B}(i\nabla - M)B \rangle + \frac{1}{2}D\langle \bar{B}\gamma^\mu\gamma_5\{u_\mu, B\} \rangle \\ & + \frac{1}{2}F\langle \bar{B}\gamma^\mu\gamma_5[u_\mu, B] \rangle,\end{aligned}\tag{1}$$

where

$$\begin{aligned}\nabla_\mu B &= \partial_\mu B + [\Gamma_\mu, B], \\ \Gamma_\mu &= \frac{1}{2}(u^\dagger \partial_\mu u) + (u \partial_\mu u^\dagger), \\ U &= u^2 = \exp(i\frac{\sqrt{2}\Phi}{f}), \\ u_\mu &= iu^\dagger \partial_\mu U u^\dagger.\end{aligned}\tag{2}$$

B and Φ represent baryon and pseudoscalar fields, respectively:

$$\begin{aligned} B &= \begin{pmatrix} \frac{1}{\sqrt{2}}\Sigma^0 + \frac{1}{\sqrt{6}}\Lambda & \Sigma^+ & p \\ \Sigma^- & -\frac{1}{\sqrt{2}}\Sigma^0 + \frac{1}{\sqrt{6}}\Lambda & n \\ \Xi^- & \Xi^0 & -\frac{2}{\sqrt{6}}\Lambda \end{pmatrix}, \\ \Phi &= \begin{pmatrix} \frac{1}{\sqrt{2}}\pi^0 + \frac{1}{\sqrt{6}}\eta & \pi^+ & K^+ \\ \pi^- & -\frac{1}{\sqrt{2}}\pi^0 + \frac{1}{\sqrt{6}}\eta & K^0 \\ K^- & \bar{K}^0 & -\frac{2}{\sqrt{6}}\eta \end{pmatrix}. \end{aligned} \quad (3)$$

The coefficients F and D denote the reduced matrix elements for semileptonic decays of octet baryons in $SU(3)$ flavor symmetry. f in the U field is the meson decay constant [13], and $\langle \dots \rangle$ denotes the trace over $SU(3)$ flavor space. Since we are interested in s -wave scattering at low energies, we need only the terms of order $\mathcal{O}(p)$ in the expansion of the U field:

$$\mathcal{L}_{MB}^1 = \frac{i}{4f^2} \langle \bar{B} \gamma^\mu [(\Phi \partial_\mu \Phi - \partial_\mu \Phi \Phi) B - B(\Phi \partial_\mu \Phi - \partial_\mu \Phi \Phi)] \rangle. \quad (4)$$

The Lagrangian in Eq. (4) is also known as the venerable Weinberg-Tomozawa term. The corresponding pseudo-potentials can be easily obtained as:

$$V_{ij} = -\frac{C_{ij}}{4f^2} \bar{u}(p_j) \gamma_\nu u(p_i) (k_i^\nu + k_j^\nu), \quad (5)$$

where p_i and p_j (k_i and k_j) are initial and final baryon (meson) momenta, respectively. The subscripts i and j denote the indices representing the coupled-channel states. The coefficients C_{ij} are derived from Eq. (4). Explicit forms of the C_{ij} for $S = -1$ and $S = 0$ are given in Refs. [7, 14].

The next step is to solve the Bethe-Salpeter(BS) equation. The general T matrix in the coupled-channel formalism is given by

$$T_{ij} = V_{ij} + \sum_l i \int \frac{d^4 q}{(2\pi)^4} \frac{V_{il}(\not{p}_l + M_l) T_{lj}}{\{(P - q)^2 - M_l^2\}(q^2 - m_l^2)}, \quad (6)$$

where M_l and m_l represent the octet baryon and meson masses in the intermediate state, respectively. P designates the total momentum given by $p + q = (\sqrt{s}, 0, 0, 0)$ in the center of mass system, where p and q denote the intermediate baryon and meson momenta, respectively. Having utilized the on-mass-shell factorization or N/D method, Eq. (6) becomes an analytically solvable and pure algebraic equation:

$$T_{ij} = V_{ij} + \sum_l V_{il} \left\{ i \int \frac{d^4 q}{(2\pi)^4} \frac{2M_l}{\{(P - q)^2 - M_l^2\}(q^2 - m_l^2)} \right\} T_{lj}. \quad (7)$$

The pseudo-potential in Eq. (7) is then written by

$$V(\sqrt{s})_{ij} = -\frac{C_{ij}}{4f^2}(\sqrt{s} - M_i - M_j)\sqrt{\frac{M_i + E_i}{2M_i}}\sqrt{\frac{M_j + E_j}{2M_j}}, \quad (8)$$

where E_i stands for the i th baryon energy.

In order to solve the BS scattering equation, we have to introduce the regularization to remove the divergence. We first use the dimensional regularization (DIM) as in Refs. [7, 15, 16]. For convenience without loss of generality, the indices representing the coupled channels will be omitted from now on. Employing the dimensional regularization, we obtain the familiar result for the two-body propagator [8]:

$$G(\sqrt{s})_{\text{DIM}} = \frac{2M}{16\pi^2} \left\{ \frac{m^2 - M^2 + s}{2s} \ln \frac{m^2}{M^2} + \frac{\xi}{2s} \ln \frac{M^2 + m^2 - s - \xi}{M^2 + m^2 - s + \xi} \right\} + \frac{2M}{16\pi^2} \ln \frac{M^2}{\mu^2}, \quad (9)$$

where

$$\xi = \sqrt{(M^2 - m^2 - s)^2 - 4sm^2} = \sqrt{(s - (M - m)^2)(s - (M + m)^2)}$$

related to on-shell center of mass momentum of meson-baryon system, $\xi/(2\sqrt{s})$. Also it is related to the phase space ($\rho = \frac{M\xi}{4s\pi}$) or the flux factor which governs the imaginary part of the T -matrix. μ stands for the renormalization scale, which contains information on the divergence of $G(\sqrt{s})$ with the minimal subtraction.

Now, we introduce form factors instead of the dimensional regularization. The form factors encode the complicated extended structure of hadrons and are usually parameterized in the form of:

$$F(q^2) = \left(\frac{\Lambda^2 - m^2}{\Lambda^2 - q^2} \right)^n, \quad (10)$$

where Λ denotes a four dimensional cut-off parameter. In the case of $n = 1$, *i.e.* monopole type of the form factor (MF), it is equivalent to the well-known *Pauli-Villars* regularization. The loop integral with the monopole type of the form factor can be performed analytically:

$$\begin{aligned} G(\sqrt{s})_{\text{MF}} &= \int \frac{d^4q}{(2\pi)^4} \frac{2M}{\{(P - q)^2 - M^2\}(q^2 - m^2)} \frac{(\Lambda^2 - m^2)}{(\Lambda^2 - q^2)} \\ &= \frac{2M}{16\pi^2} \left\{ \frac{m^2 - M^2 + s}{2s} \ln \frac{m^2}{M^2} + \frac{\xi}{2s} \ln \frac{M^2 + m^2 - s - \xi}{M^2 + m^2 - s + \xi} \right. \\ &\quad + \frac{(M^2 - m^2 - s)}{2s} \ln \frac{\Lambda^2}{M^2 - m^2 + \Lambda^2} - \ln \frac{M^2 - m^2 + \Lambda^2}{M^2} \\ &\quad \left. - \frac{\eta}{2s} \ln \frac{M^2 - m^2 - s + 2\Lambda^2 - \eta}{M^2 - m^2 - s + 2\Lambda^2 + \eta} \right\}, \end{aligned} \quad (11)$$

where

$$\eta = \sqrt{(M^2 - m^2 - s)^2 - 4s\Lambda^2}. \quad (12)$$

Though the $G(\sqrt{s})_{\text{MF}}$ shows a similar structure to $G(\sqrt{s})_{\text{DIM}}$ in Eq. (9), their analytic behaviors are rather different. It is straightforward to calculate all the cases of $n \geq 1$ by using the following recursion formula:

$$G_{n+1}(\sqrt{s}) = G_n(\sqrt{s}) - \frac{\Lambda^2 - m^2}{2n\Lambda} \frac{\partial}{\partial \Lambda} G_n(\sqrt{s}). \quad (13)$$

For example, the analytic form of $G(\sqrt{s})_{\text{DF}}$ for the dipole-type form factor ($n = 2$) becomes

$$G(\sqrt{s})_{\text{DF}} = G(\sqrt{s})_{\text{MF}} - \frac{M(\Lambda^2 - m^2)}{8\pi^2} \left\{ \frac{1}{\eta} \ln \frac{M^2 - m^2 - s + 2\Lambda^2 - \eta}{M^2 - m^2 - s + 2\Lambda^2 + \eta} \right\}. \quad (14)$$

The divergence can be canceled again by introducing the counter terms with a subtraction parameter a :

$$G \rightarrow G + \frac{2M}{16\pi^2} a, \quad (15)$$

In coupled channel calculations, G and a are diagonal elements of a matrix in the meson-baryon channels. The subtraction parameter a in Eq. (15) change only the real part of $G(\sqrt{s})$, while the imaginary part should be independent of regularization schemes, since it is finite as is constrained by unitarity.

We plot the real part of $G(\sqrt{s})$ with the DIM, DF, and MF for four different channels, *i.e.* πN and $\pi \Sigma$ without the subtraction parameters in Fig. 1. Here, we use $\mu = 1200$ MeV for the DIM, whereas $\Lambda = 1000$ MeV for the DF and MF. Thus, we can minimize the difference the between regularization schemes by fitting the subtraction parameters. However, the results turn out to be different above the thresholds.

In order to find resonances in each channel, we have to look for the corresponding poles in the second Riemann sheet. Since the pseudo-potential is real as given in Eq. (8), the poles in the second Riemann sheet are effected only by $G(\sqrt{s})$. The analytic structure of the two-body propagator is as follows:

$$\begin{aligned} G(z)_{\text{2nd}} &= G(z)_{\text{1st}}, \quad \text{for } \sqrt{s} < M + m, \\ G(z)_{\text{2nd}} &= G(z)_{\text{1st}} - 2i\text{Im}G(z)_{\text{1st}}, \quad \text{for } \sqrt{s} \geq M + m, \end{aligned} \quad (16)$$

where z stands for the total energy on the complex plane. Since the cut starts from the threshold points, the imaginary part of $G(z)$ can be obtained by the discontinuity along the

cut $\sqrt{s} > M + m$:

$$\text{Im}G(\sqrt{s}) = \frac{\rho}{2} = \frac{M\xi}{8\pi s}. \quad (17)$$

In the case of the DIM, we find exactly the same expression for the $\text{Im}G(\sqrt{s})$ by taking the imaginary part of Eq.(9) as in Ref.[14]. However, we have two complex variables, *i.e.* ξ and η give two different branch cuts which start from the points of $\sqrt{s} = M + m$ and where Eq.(12) equals zero in the region of $1 \text{ GeV} \sim 2 \text{ GeV}$ in the case of the form-factor regularizations. Hence, we have to take into account these two variables to find the poles in the second Riemann sheet. The variable η must be pure imaginary so that Eq.(17) may be satisfied. While the on-mass-shell approximation given in Eq. (7) works perfectly well for the DIM, it is to some extent limited for the form-factor regularization. However, since we are interested in resonances in the region of $1 \text{ GeV} \sim 2 \text{ GeV}$, in which η becomes pure imaginary as shown in Fig. 2, the unitarity condition is also well satisfied in the present case. Therefore, the term with η (η term) in Eq.(11) becomes pure real in the region of $1 \text{ GeV} \sim 2 \text{ GeV}$. For experimental data of $S = 0$ and $S = -1$ we use Refs. [17, 18, 19, 20, 21, 22, 23, 24, 25, 26, 27, 28].

III. NUMERICAL RESULTS OF $S = 0$ MESON-BARYON SECTOR

We start with the $S = 0$ meson-baryon sector from which $N^*(1535)$ ($I = 1/2$) [29] and $\Delta(1620)$ ($I = 3/2$) resonances arise. In Table.I we list the possible coupled channels. We fix the parameters to describe the $S = 0$ sector as follows: We choose the meson decay constants according to the empirical data $f_\pi = 93.0 \text{ MeV}$, $f_\eta = 120.9 \text{ MeV}$, and $f_K = 113.46 \text{ MeV}$. The renormalization point for the DIM is set to be $\mu = 1200 \text{ MeV}$ and the cut-off parameter is fixed to be $\Lambda = 1000 \text{ MeV}$ for the DF and MF. We use the subtraction parameters for the DIM, DF and MF as given in Table.II. While we take the subtraction parameters for the DIM from Ref. [14], we determine them for the MF and DF in such a way that the threshold-point values of $G(\sqrt{s})$ are equal to those of the DIM in order to keep consistency with chiral perturbation theory, which describes the amplitudes at low energies well.

In order to look into the characteristics of resonances, we need to investigate the partial-wave amplitudes. In order to compare the present results with the experimental data, we

normalize the transition amplitudes as follows:

$$-\sqrt{\frac{M_i \xi_i}{4\pi\sqrt{s}}}\sqrt{\frac{M_j \xi_j}{4\pi\sqrt{s}}}T(\sqrt{s})_{ij}. \quad (18)$$

Fig.3 represents the partial-wave amplitudes for πN scattering in the S_{11} and S_{31} channels. We find that the results with the MF and DF are similar to those with the DIM. The kink around 1500 MeV implies the resonance of $N^*(1535)$. Hence, $N^*(1535)$ is dynamically generated in the form-factor regularization as well as in the dimensional one, once the subtraction parameters a_i are properly chosen. However, the present calculation fails to reproduce the higher resonance $N^*(1650)$. Concerning $N^*(1650)$, we mention that Ref. [16] has reproduced it by introducing more parameters than the present work. Thus, in the present framework, using the lowest-order Chiral Lagrangian with the on-mass-shell approximation is not enough to generate the $N^*(1650)$ resonance dynamically.

In Fig.4, we draw the total cross sections of $\pi^- p$ as functions of the laboratory momentum of π^- . Both regularization schemes describe them qualitatively well. However, there is some difference in detail, which is due to the fact that the corresponding propagators shown in Fig. 1 have different slopes as the energy increases. In particular, the total cross section of the $\pi^- p \rightarrow K^0 \Sigma^0$ shows a noticeable dependence on regularizations.

Now, we are in a position to look for the poles corresponding to the resonances in each channel of the $S = 0$, $I = 1/2$ meson-baryon sector. In order to find the pole corresponding to the resonances, we need to extend the T matrix to the complex energy plane in which the propagator has a cut starting from the threshold energy.

We find that the pole is located at $(1516 - 37i)$ MeV in the case of the DIM, while those with the DF and MF are at $(1502 - 41i)$ MeV and at $(1517 - 41i)$ MeV, respectively. These results are qualitatively similar to those in Ref. [14], where two pions channel and ρ meson exchange are also included.

We can express an approximated form of the T -matrix amplitude near the pole as follows:

$$T_{ij} \simeq \frac{g_i g_j}{z - z_R}, \quad (19)$$

where the residue g_i denotes the coupling strength to the resonance in the i th channel. Hence, we can easily determine the coupling strength of the resonance, using Eq.(19). The coupling strengths of $N^*(1535)$ to each channel of $S = 0, I = 1/2$ are listed in Table III. We

find the following tendency of the coupling strengths:

$$|g_{\pi N}| < |g_{K\Lambda}| \sim |g_{\eta N}| < |g_{K\Sigma}| \quad (20)$$

for all regularizations. With these results we can conclude that the $N^*(1535)$ resonance is strongly coupled to the $K\Sigma$ channel [29]. It is interesting to compare the above results with those in Ref. [14]. While almost all channels are similar to Ref. [14], we get larger value of $|g_i|$ for the $K\Sigma$ channel as quoted in Ref. [29]. The reason lies in the fact that the $\pi\pi N$ channel may bring down the coupling strength of the $K\Sigma$ channel.

IV. NUMERICAL RESULTS OF $S = -1$ MESON-BARYON SECTOR

In this section, we investigate the $S = -1$ sector, emphasizing on the resonances $\Lambda(1405)$ ($I = 0$) and $\Lambda(1670)$ ($I = 0$) in S wave. The $\Lambda(1405)$ and $\Lambda(1670)$ resonances have already been studied in Refs. [7, 15] in the chiral unitary model in which it was shown that $\Lambda(1405)$ depends weakly on the choice of subtraction parameters while $\Lambda(1670)$ is very sensitive to them [15]. The fitting procedure is similar to that in Section III. We use $\mu = 630$ MeV for the DIM and $\Lambda = 1000$ MeV for the DF, and MF. The average meson decay constant $f = 107.18$ MeV for $S = -1$ is adopted for all regularizations as in Ref. [7]. The fitted subtraction parameters are given in Table IV, where those of the DIM are taken from Ref. [15].

In the $S = -1$, $I = 0$ sector it is of great importance to look into the $\pi\Sigma$ mass distribution around the threshold of $\bar{K}N$ (~ 1432 MeV), since the $\Lambda(1405)$ resonance arises from it. Fig. 5 shows the $\pi\Sigma$ mass distribution corresponding to the $\Lambda(1405)$ resonance. As shown in Fig. 5, the peak is well reproduced as compared to the experimental data [18]. There is almost no difference between regularizations.

The cross sections of the $S = -1$, $I_3 = 0$ are plotted in Fig.6 as functions of the lab momentum for K^-p scattering. The results are in a fairly good agreement with experimental data. While difference between regularizations is found in the $K^-p \rightarrow K^-p$, $K^-p \rightarrow \bar{K}^0 n$, and $K^-p \rightarrow \pi^- \Sigma^+$ processes, there seems no dependence on the regularization in the case of the $K^-p \rightarrow \bar{K}^0 n$ and $K^-p \rightarrow \pi^0 \Lambda$ processes.

We find three different poles in the scattering amplitude in the $S = -1$, $I = 0$ channel. In particular the two poles around ~ 1400 MeV have been confirmed in recent studies based on

the chiral unitary model [30, 31, 32, 33, 34]. In Table V and Table IV we list the positions of the poles and coupling strength as done in Section III. Three different regularizations give almost the same results.

In the $S = -1$, $I = 0$ channel, the tendency of the coupling strengths are as follows:

$$|g_{K\Xi}| < |g_{\eta\Lambda}| < |g_{\bar{K}N}| < |g_{\pi\Sigma}| \text{ for pole 1,}$$

$$|g_{K\Xi}| < |g_{\eta\Lambda}| \sim |g_{\pi\Sigma}| < |g_{\bar{K}N}| \text{ for pole 2,}$$

$$|g_{\pi\Sigma}| < |g_{\bar{K}N}| < |g_{\eta\Lambda}| < |g_{K\Xi}| \text{ for pole 3.}$$

V. DISCUSSION AND SUMMARY

We have investigated $S = 0$ and $S = -1$ meson-baryon scattering, in particular, focusing on their dependence on regularizations. Starting from the effective chiral Lagrangian to the lowest order of the chiral expansion \mathcal{L}_{MB}^1 , also known as the Weinberg-Tomozawa term, we have constructed the pseudo-potential which is used as a kernel of the Bethe-Salpeter equation. In order to solve the Bethe-Salpeter equation, we utilize the on-mass-shell approximation. While the dimensional regularization is widely adopted in almost all works, we introduced three different schemes of the regularization: The dimensional regularization, the monopole type form factor (MF), and the dipole type form factor (DF).

We examined first the dependence of the propagators on regularizations. While there is basically no difference among the regularizations in low-energy regions (below 1500 MeV), we found that in higher-energy regions (above 1500 MeV) the propagator with the dimensional regularization differs substantially from that with the monopole and dipole-type form factors. We fixed the subtraction parameters for the MF and DF at the threshold point. In addition, we used empirical values of the branching ratio and the partial wave amplitudes to fit the $S = -1$ and $S = 0$ subtraction parameters for the form-factor regularizations. For the form factor regularizations, we have found that the on-mass-shell approximation is limited to the energy region lower than a certain energy due to the appearance of an unphysical branch cut. Therefore further study with the BS scattering equation solved numerically is necessary.

We first calculated the partial-wave amplitudes for the $S = 0$ meson-baryon sector for $I = 1/2$ and $I = 3/2$. Though there exists difference between regularizations in higher-energy regions, the results were almost the same below 1500 MeV. The reason lies in the fact

that the propagator in the Bethe-Salpeter equation is rather sensitive to the regularization schemes in higher-energy region. We also calculated the total cross sections for the $S = 0$ meson-baryon sector. While all three regularizations describe well them qualitatively, we found noticeable difference between regularizations in the total cross section of $\pi^- p \rightarrow K^0 \Sigma^0$. The position of the resonance $N^*(1535)$ is similar to each other in all regularization schemes. However, the coupling strengths of $N^*(1535)$ is rather sensitive to regularizations.

The resonance $\Lambda(1405)$ in the $S = -1$ meson-baryon sector was well reproduced in the present work and turned out to be rather insensitive to the types of regularizations apart from small difference in higher-energy region. We also investigated the analytic structure of the partial-wave amplitudes and found that three poles exist in them.

The regularization dependence of the total cross sections become different according to the channels. While the processes $K^- p \rightarrow K^- p$, $K^- p \rightarrow \bar{K}^0 n$, and $K^- p \rightarrow \pi \Sigma^+$ depend on the regularization schemes, even in lower momentum region, those of $K^- p \rightarrow \pi^0 \Sigma^0$ and $K^- p \rightarrow p \rightarrow \pi^+ \Sigma^-$ show almost no dependence on regularizations. The process $K^- p \rightarrow \pi^0 \Lambda$ is changed by regularizations only in higher momentum region. The coupling strengths strongly depend on regularizations as in the $S = -1$, $I = 0$ meson-baryon sector.

In the present work, we examined the dependence of meson baryon scattering on regularization schemes. We employed three different regularizations: The dimensional regularization, the form factor regularizations with monopole and dipole types. The differences due to regularizations found in observables are mainly due to the different behavior of the propagator $G(\sqrt{s})$, because of which in higher energy region the regularizations change the prediction of the observables. Thus, we conclude that one needs to vindicate methods used so far to describe meson-baryon processes.

Acknowledgments

HCK is grateful to H. Toki for the warm hospitality at RCNP. The work of HCK is supported by the KOSEF (R01-2001-00014). The works of SINam has been supported by scholarship of the Ministry of Education, Sciences, Sports and Culture of Japan.

-
- [1] G. E. Brown, C. H. Lee, M. Rho and V. Thorsson, Nucl. Phys. A **567** (1994) 937
 - [2] C. H. Lee, H. Jung, D. P. Min and M. Rho, Phys. Lett. B **326** (1994) 14
 - [3] N. Kaiser, P. B. Siegel and W. Weise, Nucl. Phys. A **594** (1995) 325
 - [4] B. Krippa and J. T. Londergan, Phys. Rev. C **58** (1998) 1634
 - [5] R.J. Nowak *et al.*, Nucl. Phys. **B139** (1978) 61.
 - [6] D.N. Tovee *et al.*, Nucl. Phys. **B33** (1971) 493.
 - [7] E. Oset and A. Ramos, Nucl. Phys. A **635** (1998) 99
 - [8] J. A. Oller and U. G. Meissner, Phys. Lett. B **500**, 263 (2001)
 - [9] M. F. M. Lutz and E. E. Kolomeitsev, Nucl. Phys. A **700** (2002) 193
 - [10] R. Machleidt, K. Holinde and C. Elster, Phys. Rept. **149** (1987) 1.
 - [11] A. Mueller- Groeling, K. Holinde and J. Speth, Nucl. Phys. A **513** (1990) 557.
 - [12] U. G. Meissner, Rept. Prog. Phys. **56** (1993) 903
 - [13] J. Gasser and H. Leutwyler, Nucl. Phys. B **250** (1985) 465.
 - [14] T. Inoue, E. Oset and M. J. Vicente Vacas, Phys. Rev. C **65**, 035204 (2002)
 - [15] E. Oset, A. Ramos and C. Bennhold, Phys. Lett. B **527** (2002) 99 [Erratum-ibid. B **530** (2002) 260]
 - [16] J. Nieves and E. Ruiz Arriola, Phys. Rev. D **64** (2001) 116008
 - [17] G. P. Gopal, R. T. Ross, A. J. Van Horn, A. C. McPherson, E. F. Clayton, T. C. Bacon and I. Butterworth [Rutherford-London Collaboration], Nucl. Phys. B **119** (1977) 362.
 - [18] R. J. Hemingway, Nucl. Phys. B **253** (1985) 742.
 - [19] J. C. Hart *et al.*, Nucl. Phys. B **166** (1980) 73.
 - [20] D. H. Saxon *et al.*, Nucl. Phys. B **162** (1980) 522.
 - [21] R. D. Baker *et al.*, Nucl. Phys. B **145** (1978) 402; Nucl. Phys. B **141** (1978) 29.
 - [22] D. W. Thomas, A. Engler, H. E. Fisk and R. W. Kraemer, Nucl. Phys. B **56** (1973) 15.
 - [23] T. S. Mast, M. Alston-Garnjost, R. O. Bangerter, A. S. Barbaro-Galtieri, F. T. Solmitz and R. D. Tripp, Phys. Rev. D **14** (1976) 13.
 - [24] R. O. Bangerter, M. Alston-Garnjost, A. Barbaro-Galtieri, T. S. Mast, F. T. Solmitz and R. D. Tripp, Phys. Rev. D **23** (1981) 1484; Phys. Rev. D **11** (1975) 3078.
 - [25] M. Sakitt, T. B. Day, R. G. Glasser, N. Seeman, J. H. Friedman, W. E. Humphrey and

- R. R. Ross, Phys. Rev. **139** (1965) B719.
- [26] J. J. Jones *et al.*, Phys. Rev. Lett. **26** (1971) 860.
- [27] T. O. Binford, M. L. Good, V. G. Lind, D. Stern, R. Krauss and E. Dettman, Phys. Rev. **183** (1969) 1134.
- [28] O. Van Dyck *et al.*, Phys. Rev. Lett. **23** (1969) 50.
- [29] N. Kaiser, P. B. Siegel and W. Weise, Phys. Lett. B **362**, 23 (1995)
- [30] T. Hyodo, S. I. Nam, D. Jido and A. Hosaka, Phys. Rev. C **68**, 018201 (2003)
- [31] C. Garcia-Recio, J. Nieves, E. Ruiz Arriola and M. J. Vicente Vacas, Phys. Rev. D **67**, 076009 (2003)
- [32] D. Jido, J. A. Oller, E. Oset, A. Ramos and U. G. Meissner, arXiv:nucl-th/0303062.
- [33] T. Hyodo, S. i. Nam, D. Jido and A. Hosaka, arXiv:nucl-th/0305011.
- [34] T. Hyodo, A. Hosaka, E. Oset, A. Ramos and M. J. Vicente Vacas, arXiv:nucl-th/0307005.

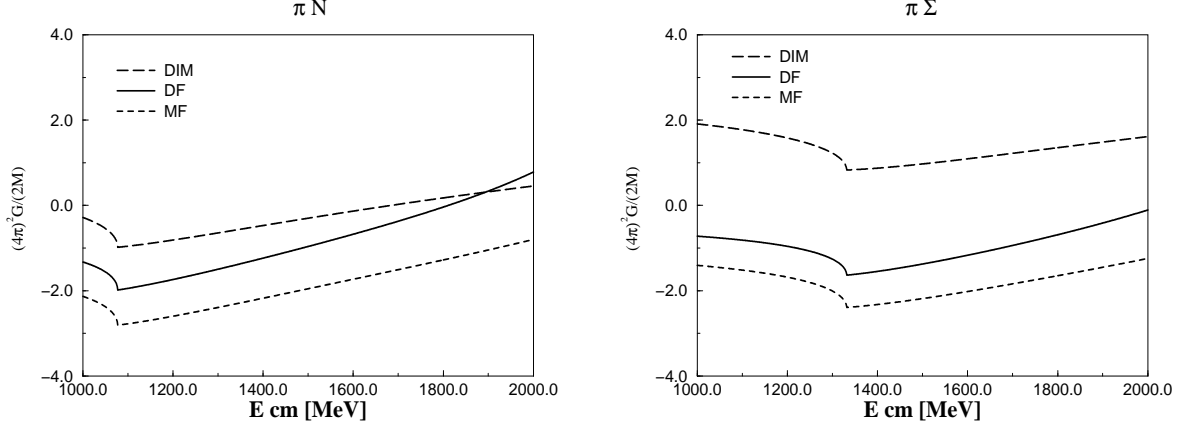


FIG. 1: The real parts of the meson-baryon loop integrals for πN ($S = -1$, $I = 0$) and $\pi\Sigma$ ($S = 0$, $I = 1/2$) channels as functions of the center of mass energy $E_{\text{cm}} (= \sqrt{s})$ for DF (solid), MF (dotted) and DIM (dashed).

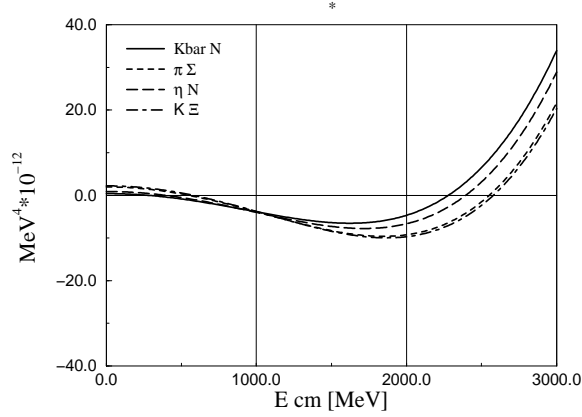


FIG. 2: $\eta^2 \times 10^{-12}$ as functions of E_{cm} for $\bar{K}N$ (solid), $\pi\Sigma$ (dotted), ηN (dashed) and $K\Xi$ (dot-dashed) channels.

TABLE I: $S = 0$ channels

	1	2	3	4
$I = 1/2$	πN	ηN	$K\Lambda$	$K\Sigma$
$I = 3/2$	πN	$K\Sigma$	-	-

TABLE II: Subtraction parameters for $S = 0$ meson-baryon sector for the DIM, DF and MF

	πN	ηN	$K\Lambda$	$K\Sigma$
DIM	2.0	0.2	1.6	-2.8
DF	3.00	0.93	2.38	-1.87
MF	3.83	1.73	3.26	-1.12

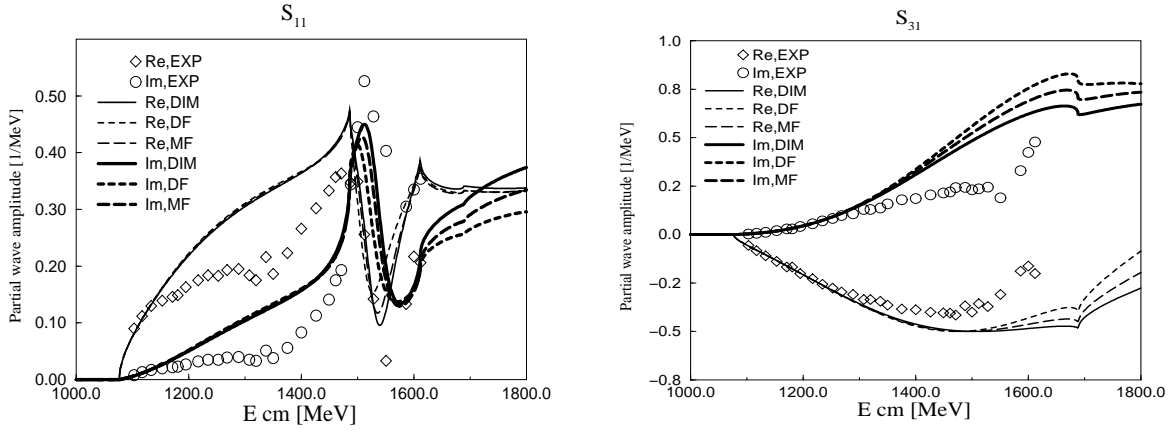


FIG. 3: πN scattering amplitudes ($S = 0$) for S_{11} and S_{31} channels as functions of the center of mass energy. Thin and Thick curves are for real and imaginary parts, where the solid, dotted and dashed ones for DIM, DF and MF, respectively. Experimental data are shown by diamonds for the real parts and by circles for the imaginary parts.

TABLE III: Coupling strengths $|g_i|$ of $N^*(1535)$ to four different channels.

	πN	ηN	$K\Lambda$	$K\Sigma$
DIM	0.46	1.79	1.09	5.17
DF	0.84	1.93	1.60	3.23
MF	1.00	2.02	1.78	3.54

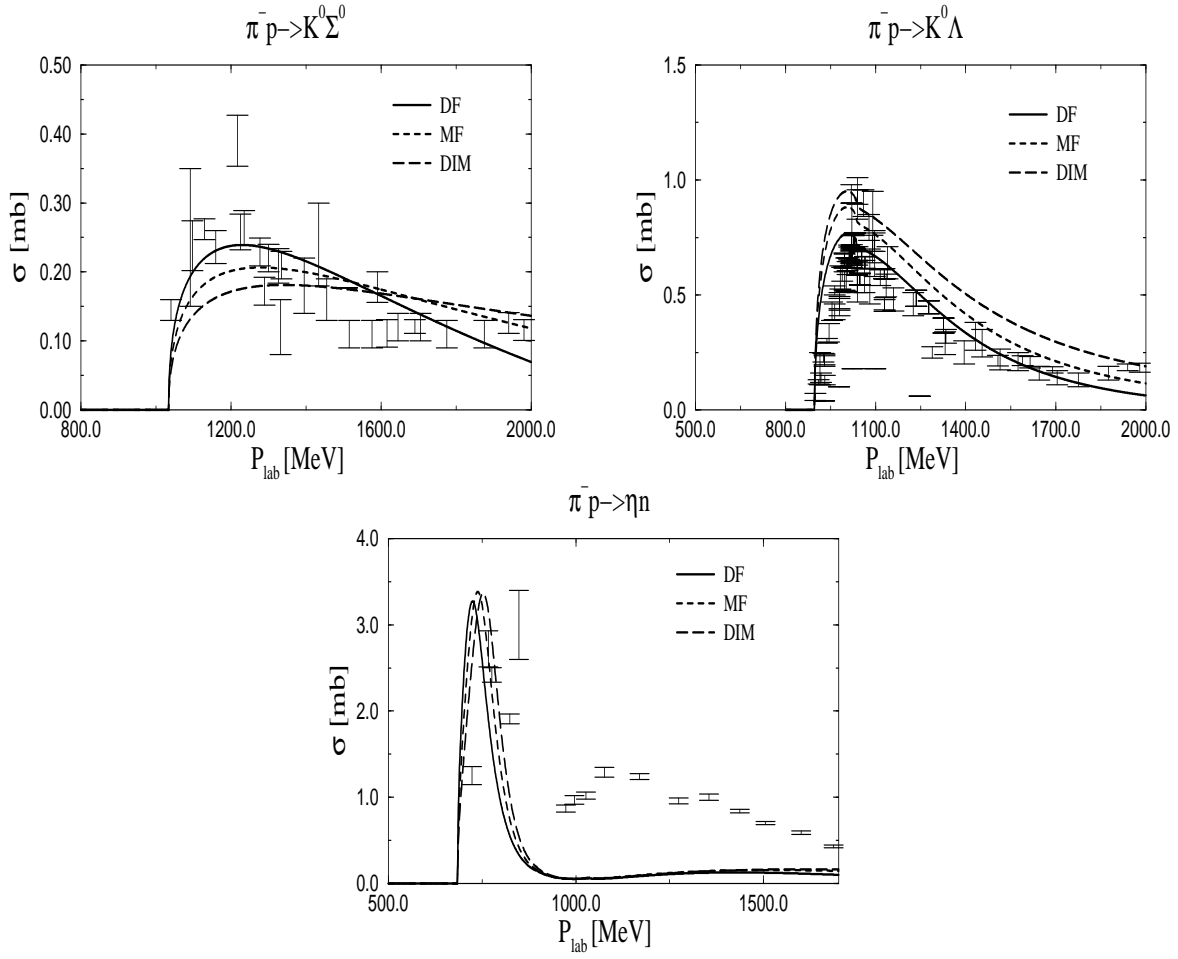


FIG. 4: $S = 0$, $I_3 = -1/2$ cross sections with different regularizations for $\pi^- p \rightarrow K^0 \Sigma^0$, $K^0 \Lambda$, and ηn as functions of the lab momentum P_{lab} . The solid curves are for the DF, the dotted one for the MF, and the dashed one for the DIM, respectively.

TABLE IV: Subtraction parameters a for the $S = -1$ meson-baryon sector for the DIM, DF and MF.

	$a_{\bar{K}N}$	$a_{\pi\Lambda}$	$a_{\pi\Sigma}$	$a_{\eta\Lambda}$	$a_{\eta\Sigma}$	$a_{K\Xi}$
DIM	-1.84	-1.83	-2.00	-2.25	-2.38	-2.67
DF	0.22	0.59	0.47	-0.12	-0.20	-0.36
MF	1.03	1.36	1.22	0.64	0.54	0.36

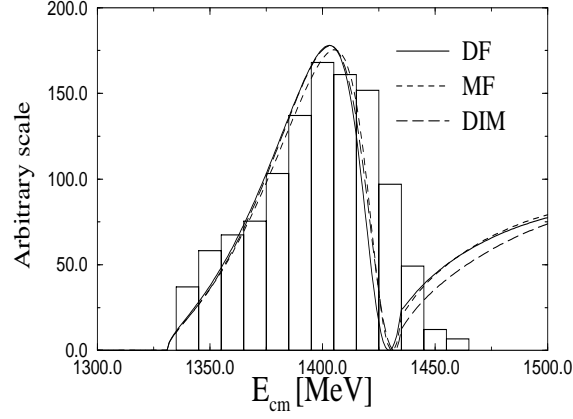


FIG. 5: $\pi\Sigma$ mass distribution around the $\Lambda(1405)$ resonance. The solid curve represents the case of the DM, while the dashed and dot-dashed ones correspond to the case of the DIM and MF, respectively. Experimental data is taken from Ref. [22].

TABLE V: Poles of the scattering amplitude in the $S = -1$ and $I = 0$ channel.

	Pole 1 (MeV)	Pole 2 (MeV)	Pole 3 (MeV)
DIM	$1398 - 74i$	$1429 - 14i$	$1688 - 22i$
DF	$1392 - 74i$	$1422 - 18i$	$1663 - 9i$
MF	$1394 - 74i$	$1425 - 17i$	$1671 - 25i$

TABLE VI: Coupling strengths $|g_{ii}|$ for three poles.

		$\bar{K}N$	$\pi\Sigma$	$\eta\Lambda$	$K\Xi$
DIM	Pole 1	1.43	2.06	0.54	0.45
	Pole 2	2.52	1.30	1.32	0.29
	Pole 3	0.68	0.16	0.98	3.14
DF	Pole 1	2.00	2.54	0.78	0.62
	Pole 2	3.64	1.83	1.82	0.53
	Pole 3	0.45	0.18	0.93	2.23
MF	Pole 1	2.65	3.57	1.01	0.83
	Pole 2	3.39	1.80	1.73	0.48
	Pole 3	1.17	0.36	1.53	4.87

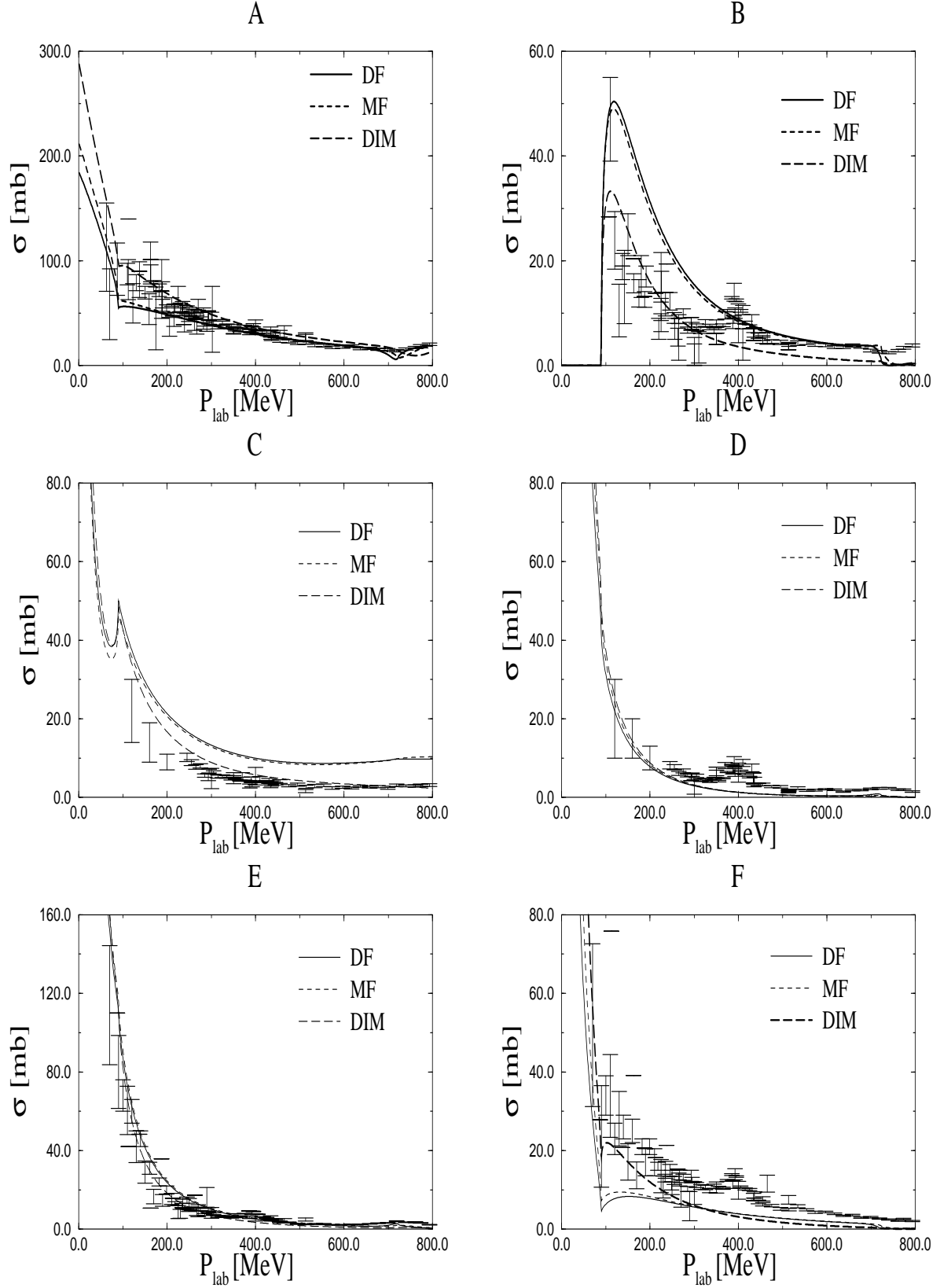


FIG. 6: $S = -1$, $I_3 = 0$ cross sections with different regularizations for $K^-p \rightarrow K^-p$, $\bar{K}^0 n$, $\pi^0\Lambda$, $\pi^0\Sigma^0$, $\pi^+\Sigma^-$, $\pi^-\Sigma^+$ as functions of the lab momentum P_{lab} . The solid curves are for the DF, the dotted one for the MF, and the dashed one for the DIM, respectively.